INTERNATIONAL JOURNAL FOR NUMERICAL METHODS IN FLUIDS, VOL. 9, 1145–1164 (1989)

A FAST RIEMANN SOLVER WITH CONSTANT COVOLUME APPLIED TO THE RANDOM CHOICE METHOD

E. F. TORO

Department of Aerodynamics, Cranfield Institute of Technology, Cranfield, Bedfordshire MK43 0AL, U.K.

SUMMARY

The Riemann problem for the unsteady one-dimensional Euler equations together with the constant-covolume equation of state is solved exactly. The solution is then applied to the random choice method to solve the general initial-boundary value problem for the Euler equations. The iterative procedure to find p^*, the pressure between the acoustic waves, involves a single algebraic (non-linear) equation, all other quantities follow directly throughout the x–t plane, except within rarefaction fans where an extra iterative procedure is required. The solution is validated against existing exact results both directly and in conjunction with the random choice method.

KEY WORDS Riemann problem Covolume Random choice

1. INTRODUCTION

The ideal-gas kinetic theory assumes that molecules occupy a negligible volume and that they do not exert forces on one another. In applications such as in combustion processes, these assumptions are no longer accurate descriptions of the problem. In this paper we incorporate covolume; that is to say, we assume that molecules occupy a finite volume b so that the volume available for molecular motion is $v-b$. The resulting thermal equation of state is

$$p(v-b)=RT. \tag{1}$$

Here p, v, R and T are the pressure, the volume, the gas's constant and the absolute temperature respectively, with $v=1/\rho$; ρ is the density.

If one were to assume intermolecular forces as well, then the Van der Waals' equation of state would result. However, we are only interested in equation (1) where b is constant (with dimensions $m^3\,kg^{-1}$). Corner[1] reports on experimental results for a good range of solid propellants and observed that the covolume b varied very little, i.e. $0{\cdot}9\times10^{-3}\leqslant b\leqslant 1{\cdot}1\times10^{-3}\ m^3\,kg^{-1}$. The best values of b lead to errors no greater than 2% and thus we feel there is some justification in using equation (1) with $b=$constant when modelling gas dynamical events associated with solid propellant burning.

The main motivation of the present work is to extend the applicability of the random choice method (RCM) to model gas dynamical events arising from, and coupled with, combustion phenomena. Since the RCM uses the exact solution of the Riemann problem, our first task will be to devise an efficient Riemann solver. In Reference 2 we derived a number of covolume relations

0271–2091/89/091145–20$10.00

Received June 1988

and indicated a solution strategy based on the Newton–Raphson method applied to a 3×3 system of algebraic equations. For rarefaction fans we also suggested a similar approach to solve another 3×3 system. The resulting Riemann solver was found to be more efficient than that based on the Godunov iteration when applied to the special case $b=0$ (ideal gas), but the net gains were limited.

The present Riemann solver is much more efficient; it is an extension of that proposed in Reference 3 for ideal gases. The two iteration procedures that are present (one for the pressure p^* between the acoustic waves and the other for the density ρ inside rarefaction fans) involve a single algebraic equation. The Newton–Raphson method works well in both cases.

The implementation of the RCM using the exact Riemann solver is carried out on a non-staggered grid, whereby the solution to the next time level is advanced in a single step. This programming strategy has a number of advantages over the more common staggered grid approach. Simplicity is one of them. Use of irregular/adaptive grids is another. The original idea appears to be due to Colella.[4]

The remaining part of this paper is organized as follows. Section 2 defines the Riemann problem and delineates the solution strategy. In Section 3 we collect the covolume relations required to solve the problem. In Section 4 we solve the Riemann problem. In Section 5 we describe the implementation of the RCM. In Section 6 we apply the solution directly and in conjunction with the RCM. Results are compared with existing exact solutions. Finally, in Section 7 we draw some conclusions and indicate areas of application of the present results.

2. THE RIEMANN PROBLEM

We consider the Riemann problem for the unsteady one-dimensional Euler equations together with the covolume equation of state (1) with constant b, namely

$$\mathbf{U}_t + \mathbf{F}(\mathbf{U})_x = 0, \tag{2}$$

$$\mathbf{U}(x, t_0) = \begin{cases} \mathbf{U}_L, & x \leqslant x_0, \\ \mathbf{U}_R, & x \geqslant x_0, \end{cases} \tag{3}$$

where $-\infty < x < \infty$ and $t > t_0$. Here $\mathbf{U} = \mathbf{U}(x, t)$ with x and t denoting space and time respectively. In equation (2) the subscripts denote partial differentiation as usual. U and $\mathbf{F}(\mathbf{U})$ are vectors of conserved variables and fluxes respectively. These are given by

$$\mathbf{U} = \begin{bmatrix} \rho \\ \rho u \\ E \end{bmatrix}, \qquad \mathbf{F}(\mathbf{U}) = \begin{bmatrix} \rho u \\ \rho u^2 + p \\ (E+p)u \end{bmatrix}, \tag{4}$$

where u is the velocity, e is the specific internal energy and E is the total energy given by

$$E = \tfrac{1}{2}\rho u^2 + \rho e. \tag{5}$$

The initial condition (3) consists of two constant states $\mathbf{U}_L$ and $\mathbf{U}_R$.

Note that equation (1) serves as a closure condition for system (2), which has three differential equations and four unknowns. A corresponding caloric equation of state gives an expression for the specific internal energy in equation (5) in terms of the unknowns of system (2).

The solution of the Riemann problem (1)–(5) for $t > t_0$ can be represented in the half x–t plane as in Figure 1.

There are three waves present: W_L, W_M and W_R. The middle wave W_M is always a contact discontinuity, the left wave W_L is either a shock or a rarefaction and the right wave W_R is either a shock or a rarefaction. Hence there are four possible wave patterns. The region star between waves

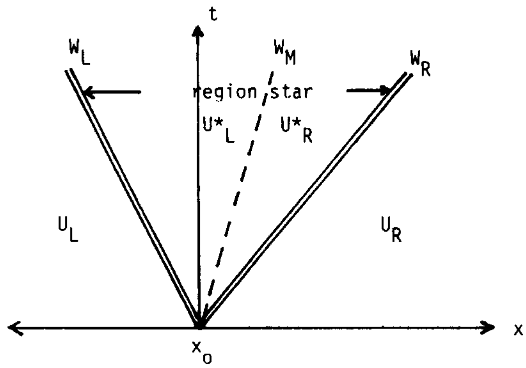

Figure 1. Solution of the Riemann problem with data $\mathbf{U}_L$ (left) and $\mathbf{U}_R$ (right) for the unsteady one-dimensional Euler equations

W_L and W_R is characterized by having pressure $p^* =$constant and velocity $u^* =$constant with $\rho = \rho_L^*$ between W_L and W_M (star left) and $\rho = \rho_R^*$ between W_M and W_R (star right). In the portion of the half x–t plane to the left of wave W_L the solution is equal to the constant state $\mathbf{U}_L$ (data). Similarly $\mathbf{U} = \mathbf{U}_R$ in the region to the right of wave W_R. The solution $\mathbf{U}$ at a time $t > t_0$ inside a rarefaction fan (W_L or W_R) varies smoothly with x.

The principal step of the solution procedure is the determination of the solution in the region star. We call this the *star step*. A feature of the present Riemann solver is that the star step consists of a single (non-linear) algebraic equation for the pressure p^*. Other quantities in the region star follow directly. Clearly, the solution for p^* must be found iteratively, since the type of waves W_L and W_R is not known *a priori*. This must be determined as part of the solution.

The star step requires equations connecting $\mathbf{U}_L$(data) to $\mathbf{U}_L^*$ and $\mathbf{U}_R$(data) to $\mathbf{U}_R^*$. In each situation one must derive equations for the case in which the connecting wave is a shock or a rarefaction. These equations are manipulated in such a way that the velocities u_L^* and u_R^* are expressed as

$$u_L^* = f_L(p^*, \mathbf{U}_L), \qquad u_R^* = f_R(p^*, \mathbf{U}_R). \tag{6}$$

But $u_L^* = u_R^*$ gives a single algebraic non-linear equation for the unknown p^*, i.e.

$$f(p^*, \mathbf{U}_L, \mathbf{U}_R) \equiv f_L(p^*, \mathbf{U}_L) - f_R(p^*, \mathbf{U}_R) = 0. \tag{7}$$

A certain amount of work is involved in determining the form of the functions f_L and f_R in equations (6) and thus f in equation (7).

Once p^* is known from equation (7), all other quantities in region star follow directly from explicit relations. If both waves W_L and W_R are shocks, then the solution of the Riemann problem has been determined everywhere in the half x–t plane. However, if a rarefaction fan is present, the solution inside it requires another iterative procedure. This is unlike the ideal-gas case, where the solution inside a rarefaction fan follows directly from the star step (also iterative). We present an economical way of finding the solution inside rarefaction fans. Instead of solving a 3×3 non-linear system (as suggested in Reference 2), we solve a single non-linear equation for the density ρ. Other quantities follow directly.

Next we collect some basic relations for shock and rarefaction waves and derive covolume expressions for the internal energy and the sound speed. These will be utilized later in the star step.

3. COVOLUME RELATIONS

Here we collect some of the covolume equations derived in Reference 2. There we showed that the specific internal energy e is given by

$$e=\frac{p(1-b\rho)}{\rho(\gamma-1)} \tag{8}$$

and the sound speed c is given by

$$c=\left(\frac{p\gamma}{\rho(1-b\rho)}\right)^{1/2}. \tag{9}$$

Here γ denotes the ratio of specific heats as usual. The derivation of equations across shocks and rarefactions is now dealt with separately.

3.1. Shock relations

Consider the case of a right-travelling shock wave of speed S_R. In the steady frame of reference attached to the shock the usual equations for mass momentum and energy apply. In Reference 2 we formulated the solution of the star step in terms of the pressure p^* and two parameters M_L and M_R. In the present paper the solution strategy is different, but expressions for M_L and M_R are still useful. For a right-moving wave (shock or rarefaction) M_R is defined as

$$M_R=\frac{p^*-p_R}{u^*-u_R}. \tag{10}$$

For a right-travelling shock the steady shock relations give

$$M_R^2=\frac{\rho_R(p^*-p_R)D_R}{D_R-1}, \tag{11}$$

where $D_R=\rho_R^*/\rho_R$ is the density ratio across the shock wave. Also, the standard Hugoniot relation can be written as

$$e^*-e_R=\tfrac{1}{2}\left(\frac{p_R}{\rho_R}\right)\left(\frac{(H_R+1)(D_R-1)}{D_R}\right), \tag{12}$$

where $H_R=p^*/p_R$ is the pressure ratio across the shock. Substitution of e from equation (8) into equation (12) gives a relationship between H_R and D_R across the shock, i.e.

$$D_R=\frac{(\gamma+1)H_R+\gamma-1}{(\gamma-1+2b\rho_R)H_R+\gamma+1-2b\rho_R}, \tag{13}$$

which, if used in equation (11), leads to

$$M_R=\left[\left(\frac{\gamma+1}{2}\frac{\rho_R p_R}{1-b\rho_R}\right)\left(H_R+\frac{\gamma-1}{\gamma+1}\right)\right]^{1/2}. \tag{14}$$

Similarly, for the left-travelling wave W_L a parameter M_L can be defined as

$$M_L=-\frac{p^*-p_L}{u^*-u_L}, \tag{15}$$

which, after using appropriate relations, becomes

$$M_{\rm L}=\left[\left(\frac{\gamma+1}{2}\frac{\rho_{\rm L}p_{\rm L}}{1-b\rho_{\rm L}}\right)\left(H_{\rm L}+\frac{\gamma-1}{\gamma+1}\right)\right]^{1/2}. \tag{16}$$

Here $H_{\rm L}=p^*/p_{\rm L}$ is the pressure ratio across the left-moving shock.

3.2. *Rarefaction relations*

In order to obtain expressions for $M_{\rm L}$ and $M_{\rm R}$ in the case in which waves $W_{\rm L}$ and $W_{\rm R}$ are rarefaction waves, we need the generalized Riemann invariants and the isentropic relations. For a left rarefaction

$$J_{\rm L}=u+\frac{2c}{\gamma-1}(1-b\rho)=\text{constant} \tag{17}$$

and

$$\frac{\rho^*_{\rm L}}{1-b\rho^*_{\rm L}}=\frac{\rho_{\rm L}}{1-b\rho_{\rm L}}H_{\rm L}^{1/\gamma}. \tag{18}$$

For a right rarefaction we have

$$J_{\rm R}=u-\frac{2c}{\gamma-1}(1-b\rho)=\text{constant} \tag{19}$$

and

$$\frac{\rho^*_{\rm R}}{1-b\rho^*_{\rm R}}=\frac{p_{\rm R}}{1-b\rho_{\rm R}}H_{\rm R}^{1/\gamma}. \tag{20}$$

Use of equations (17) and (18) gives

$$M_{\rm L}=\frac{\gamma-1}{2}\left(\frac{\rho_{\rm L}p_{\rm L}}{\gamma(1-b\rho_{\rm L})}\right)^{1/2}\frac{1-H_{\rm L}}{1-H_{\rm L}^{(\gamma-1)/2\gamma}} \tag{21}$$

and use of equations (19) and (20) gives

$$M_{\rm R}=\frac{\gamma-1}{2}\left(\frac{\rho_{\rm R}p_{\rm R}}{\gamma(1-b\rho_{\rm R})}\right)^{1/2}\frac{1-H_{\rm R}}{1-H_{\rm R}^{(\gamma-1)/2\gamma}}. \tag{22}$$

We now return to equation (6). Note that for a left wave, from definition (15) for $M_{\rm L}$ we have

$$u^*=u_{\rm L}+\frac{p_{\rm L}-p^*}{M_{\rm L}}$$

or

$$u^*=u_{\rm L}+\tilde{f}_{\rm L}(p^*_{\rm L},\mathbf{U}_{\rm L}), \tag{23}$$

where

$$\tilde{f}_{\rm L}=\begin{cases}(1-H_{\rm L})\left(\dfrac{2(1-b\rho_{\rm L})p_{\rm L}/(\gamma+1)\rho_{\rm L}}{H_{\rm L}+(\gamma-1)/(\gamma+1)}\right)^{1/2} & \text{if } H_{\rm L}\geqslant 1 \quad \text{(shock)}, \quad (24\text{a})\\[2ex] \dfrac{2(1-b\rho_{\rm L})c_{\rm L}}{\gamma-1}\left(1-H_{\rm L}^{(\gamma-1)/2\gamma}\right) & \text{if } H_{\rm L}<1 \quad \text{(rarefaction)}. \quad (24\text{b})\end{cases}$$

Similarly, for a right wave definition (10) gives

$$u^*=u_{\rm R}-\tilde{f}_{\rm R}(p^*,\mathbf{U}_{\rm R}), \tag{25}$$

where

$$\tilde{f}_{\mathrm{R}} = \begin{cases} (1-H_{\mathrm{R}})\left(\dfrac{2(1-b\rho_{\mathrm{R}})p_{\mathrm{R}}/(\gamma+1)\rho_{\mathrm{R}}}{H_{\mathrm{R}}+(\gamma-1)/(\gamma+1)}\right)^{1/2} & \text{if } H_{\mathrm{R}} \geqslant 1 \quad \text{(shock)}, \qquad (26\mathrm{a}) \\ \dfrac{2(1-b\rho_{\mathrm{R}})c_{\mathrm{R}}}{\gamma-1}\,(1-H_{\mathrm{R}}^{(\gamma-1)/2\gamma}) & \text{if } H_{\mathrm{R}} < 1 \quad \text{(rarefaction)}. \qquad (26\mathrm{b}) \end{cases}$$

We have now completely determined the problem for the *star step*. From equations (23) and (25) the single equation (7) for p^* results, where $f_{\mathrm{L}} = u_{\mathrm{L}} + \tilde{f}_{\mathrm{L}}$ and $f_{\mathrm{R}} = u_{\mathrm{R}} - \tilde{f}_{\mathrm{R}}$; $\tilde{f}_{\mathrm{L}}$ and $\tilde{f}_{\mathrm{R}}$ are given by equations (24) and (26) respectively.

4. ALGORITHM FOR THE SOLUTION OF THE RIEMANN PROBLEM

Here we use all the relations developed in Section 3 to implement an efficient algorithm for completely solving the Riemann problem with constant covolume in the half x–t plane.

As pointed out in Section 2, the solution procedure consists basically of the *star step* and the *rarefaction fan step*. The principal part of the star step is the solution of an equation for the pressure p^* in region star. The rarefaction fan step consists of finding the complete solution inside a rarefaction fan; its principal step is the solution of a single equation for the density ρ. Both steps contain an iteration. We shall deal with each of them separately.

4.1. The star step

The main part here is the determination of p^* by solving the single non-linear algebraic equation

$$f(p^*, \mathbf{U}_{\mathrm{L}}, \mathbf{U}_{\mathrm{R}}) = \tilde{f}_{\mathrm{L}}(p^*, \mathbf{U}_{\mathrm{L}}) + \tilde{f}_{\mathrm{R}}(p^*, \mathbf{U}_{\mathrm{R}}) + u_{\mathrm{L}} - u_{\mathrm{R}} = 0, \tag{27}$$

where $\tilde{f}_{\mathrm{L}}$ and $\tilde{f}_{\mathrm{R}}$ are given by equations (24) and (26) respectively. We do this by a Newton–Raphson iteration procedure of the form

$$p^*_{(k)} = p^*_{(k-1)} + \delta_{(k-1)},$$

where

$$\delta_{(k)} = -f(p^*_{(k)}, \mathbf{U}_{\mathrm{L}}, \mathbf{U}_{\mathrm{R}})/f'_{(k)}.$$

Here k denotes the iteration and $\delta_{(k)}$ is an increment at the kth iteration.

The method requires the evaluation of derivatives

$$f'_{(k)} = \frac{\mathrm{d}}{\mathrm{d}p^*} f(p^*, \mathbf{U}_{\mathrm{L}}, \mathbf{U}_{\mathrm{R}})\bigg|_{p^* = p^*_{(k)}} \tag{28}$$

at the known point $p^* = p^*_{(k)}$ and an initial (guess) value p^*_0. An economical guess value would be $p^*_0 = \frac{1}{2}(p_{\mathrm{L}} + p_{\mathrm{R}})$, but it could be inaccurate which can increase the number of iterations for convergence. We say that the iteration procedure has converged to the solution at iteration $k = K$ if

$$\mathrm{CHA} = \frac{|p^*_K - p^*_{(K-1)}|}{p^*_{(K)}} \leqslant \mathrm{TOL}, \tag{29}$$

where TOL is a chosen tolerance; e.g. $\mathrm{TOL} = 10^{-4}$ is found to give sufficiently accurate solutions.

An accurate (although expensive) guess value p_0^* can be found if we assume that both acoustic waves W_L and W_R are rarefaction waves; that is, in evaluating $\tilde{f}_L$ and $\tilde{f}_R$ in equation (27) for p^*, equations (24b) and (26b) apply. Algebraic manipulations give a closed-form solution for p_0^* as

$$p_0^* = \left(\frac{(1-b\rho_L)c_L + (1-b\rho_R)c_R + [(\gamma-1)/2](u_L - u_R)}{(1-b\rho_L)c_L/p_L^{(\gamma-1)/2\gamma} + (1-b\rho_R)c_R/p_R^{(\gamma-1)/2\gamma}} \right)^{2\gamma/(\gamma-1)} \tag{30}$$

Clearly, if both W_L and W_R are rarefaction waves, then equation (30) gives the exact solution for p^*. But even if the assumption leading to equation (30) is not true, the estimate p_0^* is quite accurate[3] even for cases involving shocks of strength of about three. The reason for this is that the rarefaction and shock branches of the p–u curve[5] have first and second continuous derivatives at their intersection point. Thus a continuation of, say, a shock branch via the rarefaction branch is a good approximation for data states $\mathbf{U}_L$ and $\mathbf{U}_R$ that are sufficiently close in a given sense.

If the solution of the Riemann problem is used in a local sense, as applied to the random choice method, then there may well be one or two genuine discontinuities (shocks or contacts) in the flow field at a given time. Thus typically 98% of the local Riemann problems have data with close states and thus p_0^* as given by equation (30) is very accurate. A single iteration is performed in most, if not all, of these cases.

Once p^* has been found, u^* follows directly from either of equations (23) or (25). In practice, it is advisable to take a mean value. The determination of ρ_L^* and ρ_R^* (Figure 1) depends now on the type of waves W_L and W_R. For instance, if W_R is a shock wave, then ρ_R^* follows directly from equation (13); if W_L is a shock wave, we use the counterpart of equation (13) to find ρ_L^*. If W_L is a rarefaction, then equation (18) gives ρ_L^*; if W_R is a rarefaction, equation (20) gives ρ_R^*. Thus the complete solution of the Riemann problem in the region star has been obtained.

A simple but important Riemann problem is that arising at boundaries. The solution has closed form and is given in the next section.

4.2. The Riemann problem at a moving boundary

Consider the right boundary and assume this is given by a piston moving with known speed V_p. If reflections are to be allowed, then the following boundary conditions apply:

$$\rho_R = \rho_L, \qquad u_R = -u_L + 2V_p, \qquad p_R = p_L. \tag{31}$$

Here the subscript L denotes the last grid point inside the computational domain and the subscript R denotes the fictitious grid point immediately to the right of the piston.

The Riemann problem with data (31) has the solution depicted in Figure 1 with $u^* = V_p$ and W_L and W_R both of the same type, i.e. both rarefactions or both shocks.

Now we find the pressure p^* explicitly. It is easy to see that the functions $\tilde{f}_L$ and $\tilde{f}_R$ in equation (27) are identical and that $\tilde{f}_L + u_L - V_p = 0$.

If $V_p > u_L$, then both W_L and W_R are rarefaction waves and the solution for p^* is

$$p^* = p_L \left(1 - \frac{(\gamma-1)(V_p - u_L)}{2(1-b\rho_L)c_L} \right)^{2\gamma/(\gamma-1)}. \tag{32}$$

If $V_p \leqslant u_L$, then both W_L and W_R are shock waves with

$$p^* = p_L \frac{2\alpha_L + (u_L - V_p)^2 + (u_L - V_p)\sqrt{[4\alpha_L(1+\beta) + (u_L - V_p)^2]}}{2\alpha_L}, \tag{33}$$

where

$$\alpha_L = \frac{2(1-b\rho_L)p_L}{(\gamma+1)\rho_L}, \qquad \beta = \frac{\gamma-1}{\gamma+1}. \tag{34}$$

For the left boundary the analysis is identical and the result is

$$p^* = p_R\left(1 - \frac{(\gamma-1)(u_R - V_p)}{2(1-b\rho_R)c_R}\right)^{2\gamma/(\gamma-1)} \tag{35}$$

if $V_p < u_R$ (two rarefactions) and

$$p^* = p_R \frac{2\alpha_R + (V_p - u_R)^2 + (V_p - u_R)\sqrt{[4\alpha_R(1+\beta) + (V_p - u_R)^2]}}{2\alpha_R} \tag{36}$$

if $V_p > u_R$ (two shocks), where α_R is given by equation (34) with ρ_L, p_L replaced by ρ_R, p_R.
The problem that remains is the determination of the solution inside rarefaction fans.

4.3. *Solution inside rarefaction fans*

We consider only one case in detail. Suppose the left-travelling wave W_L is a rarefaction wave as illustrated in Figure 2. Consider a general point $Q(\hat{x}, \hat{t})$ inside the rarefaction fan bounded by characteristics $dx/dt = u_L - c_L$ (head) and $dx/dt = u^* - c_L^*$ (tail). A characteristic ray through the origin and Q has slope $dx/dt = u - c$ in the x–t plane, where both u and c are unknowns of the problem. Then

$$u = \hat{x}/\hat{t} + c. \tag{37}$$

Use of the left Riemann invariant J_L given by equation (17) and of equation (37) gives

$$c\left(1 + \frac{2}{\gamma-1}(1-b\rho)\right) = J_L(\mathbf{U}_L) - \frac{\hat{x}}{\hat{t}}. \tag{38}$$

Now using definition (9) of sound speed and isentropic relation (18), with ρ_L^* replaced by ρ, at point Q we obtain

$$p = p_L\left(\frac{1-b\rho_L}{\rho_L}\right)^{\gamma}\left(\frac{\rho}{1-b\rho}\right)^{\gamma}. \tag{39}$$

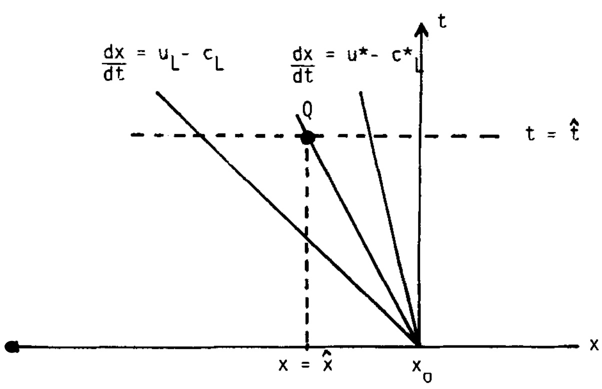

Figure 2. The sampling point $Q(\hat{x}, \hat{t})$ lies inside a left rarefaction wave. The head and tail of the wave are given by $dx/dt = u_L - c_L$ and $dx/dt = u^* - c_L^*$ respectively

Further algebraic manipulations give

$$F_L = \rho^{\gamma-1}(\gamma+1-2b\rho)^2 - \beta_L(1-b\rho)^{\gamma+1} = 0 \tag{40}$$

and

$$\partial F_L/\partial\rho = (\gamma+1)[b\beta_L(1-b\rho)^\gamma + (\gamma+1-2b\rho)(\gamma-1-2b\rho)\rho^{\gamma-2}], \tag{41}$$

where the constant β_L is given by

$$\beta_L = \frac{\{(\gamma-1)[J_L(\mathbf{U}_L) - \hat{x}/\hat{t}]\}^2}{\gamma p_L[(1-b\rho_L)/\rho_L]^\gamma}. \tag{42}$$

Equation (40) is a non-linear algebraic equation for ρ. We solve this using a combination of the Newton–Raphson and the secant methods. Once ρ is found to a given accuracy, the pressure p follows immediately from equation (39). The sound speed c is now known from equation (9) and the velocity u follows directly from equation (37).

For the case of a right rarefaction the analysis is entirely analogous. The equation for ρ inside the fan is

$$F_R = \rho^{\gamma-1}(\gamma+1-2b\rho)^2 - \beta_R(1-b\rho)^{\gamma+1} = 0, \tag{43}$$

where

$$\beta_R = \frac{\{\hat{x}/t - u_R + [2c_R/(\gamma-1)](1-b\rho_R)\}^2}{\gamma p_R[(1-b\rho_R)/\rho_R]^\gamma}. \tag{44}$$

Then p follows from an equation like equation (39) with ρ_L, p_L replaced by ρ_R, p_R. The sound speed c follows from the definition (9) and u is given by

$$u = \hat{x}/\hat{t} - c. \tag{45}$$

The exact solution of the Riemann problem with constant volume is now known everywhere in the half x–t plane (Figure 1).

5. THE RANDOM CHOICE METHOD (RCM) WITH COVOLUME

In this section we describe the way the exact solution of the Riemann problem can be used locally to obtain (numerically) the global solution of the general initial-boundary value problem for the Euler equations.

Consider the system of equations (2) in a finite domain $0 \leqslant x \leqslant L$ subject to general initial data at a time t_n, say. If the spatial domain is discretised into M cells of size Δx and the general data are approximated by piecewise-constant functions, then the original problem has been replaced by a sequence of local Riemann problems, RP(i, $i+1$) for $i = 1, \ldots, M-1$. In addition, there are two more boundary Riemann problems, RP(0, 1) and RP(M, $M+1$). Data for RP(i, $i+1$) consist of two constant states U_i^n (left) and U_{i+1}^n (right). The discrete problem is illustrated in Figure 3. Each local Riemann problem has solution as depicted in Figure 1 and can be solved exactly by the method of Section 4. Now the solution is valid locally for a restricted range of space and time, i.e. before wave interaction occurs. For a sufficiently small time increment ΔT the local solutions are unique in their respective domains so that the global solution at time $t_{n+1} = t_n + \Delta T$ is uniquely defined for $0 \leqslant x \leqslant L$. Within cell i (Figure 3) the solution is composed of the exact solutions of RP($i-1$, i) and RP(i, $i+1$). We denote this exact solution by V_i^{n+1}. Note that $V_i^{n+1}(x, t_{n+1})$ depends on $x(x_i < x < x_{i+1})$; it is not constant in general. In fact, there may be strong discontinuities transversing cell i. In order to advance the numerical solution in time, a procedure

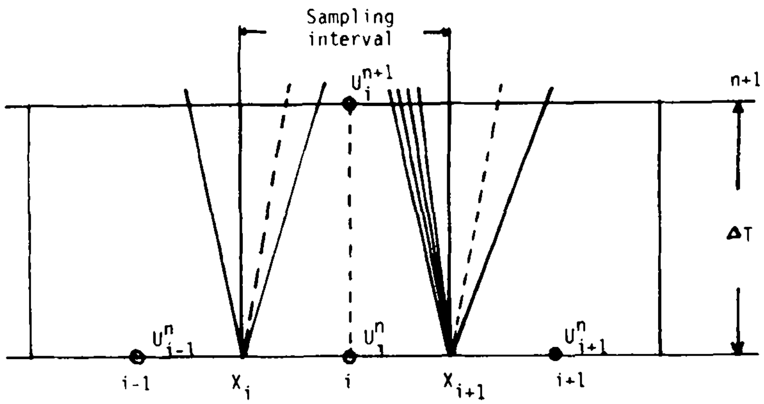

Figure 3. Solution of local Riemann problems RP($i-1$, i) and RP(i, $i+1$) determining the solution U_i^{n+1} in cell i at the new time level $n+1$. Sampling is performed in the interval $[x_i, x_{i+1}]$ of length Δx at time level $n+1$

to update U_i^n to U_i^{n+1} is required. The random choice method[4, 6] takes

$$U_i^{n+1} = V_i^{n+1}(Q_i) \tag{46}$$

where $Q_i = (x_i + \theta_n \Delta x, t_n + \Delta T)$ is a point at a 'random' position within cell i. Here θ_n is a pseudo-random number in the interval [0, 1].

We remark that a better known version of the RCM advances the solution in two steps using a staggered grid.[6] The one-step RCM on a non-staggered grid as presented here is simpler to implement and has a number of advantages over the staggered grid version. This is most evident when source terms depending on x and t are incorporated; also, when using higher-order versions,[7] hybrid schemes[8] or irregular grids,[9] the one-step RCM facilitates coding enormously.

Two more aspects of the method require attention, namely the choice of the time step size ΔT and the generation of the pseudo-random numbers θ_n. The choice of ΔT is dictated by the requirement that no waves should interact. This is the CFL condition. A popular version for the RCM is

$$\Delta T = C_S \Delta x / S_{max}, \tag{47}$$

where the coefficient C_S is chosen within the interval $(0, \frac{1}{2}]$ and S_{max} is the maximum wave speed present at time t_n, i.e.

$$S_{max} = \max(|u_i^n| + c_i^n). \tag{48}$$

The CFL condition (47) chooses ΔT in such a way that no wave is allowed to transverse more than half a cell size. This is convenient to implement, but one could do better by monitoring intersection points within each cell and then choosing ΔT appropriately.

Concerning the sequence $\{\theta_n\}$, it has been established[4] that Van der Corput sequences give the best results. Truly random numbers are not as adequate. A general Van der Corput sequence[10] $\{\theta_n\}$ depends on two parameters k_1 and k_2, with $k_1 > k_2 > 0$, both integer and relatively prime. Then the (k_1, k_2) Van der Corput sequence $\{\theta_n\}$ is formally defined as

$$\theta_n = \sum_{i=0}^{m} A_i k_1^{-(i+1)}, \tag{49}$$

where

$$A_i = k_2 a_i \pmod{k_1}, \tag{50}$$

$$n = \sum_{i=0}^{m} a_i k^i. \tag{51}$$

Equation (49) says that the nth member $\theta_n \in [0, 1]$ of the (k_1, k_2) Van der Corput sequence is a summation of m terms involving powers of k_1. The coefficients A_i are defined by equations (50) and (51). First, the non-negative integer n is expressed in the scale of notation with radix k_1 (base k_1) by equation (51), e.g. $k_1 = 2$, $k_2 = 1$ gives the binary expansion of n.

Table I contains coefficients a_i of equation (51) for $k_1 = 2$ and $k_1 = 3$ for ten values of n. The next stage is to find the 'modified' coefficients A_i from equation (50), i.e. A_i is the remainder of dividing $k_2 a_i$ by k_1 ($A_i < k_1$). The simplest case is $k_2 = 1$; then $A_i = a_i \forall_i$ (for all i). Table II(a) shows the coefficients A_i for ten values of n when $k_1 = 3$ and $k_2 = 2$. Having found A_i for $i = 0, \ldots, m$, the actual members θ_n of the sequence are computed from equation (49). Table II(b) shows the first ten members of two Van der Corput sequences.

The final stage to implement the RCM is the sampling procedure. Figure 3 shows that the updated value U_i^{n+1} depends on sampling the exact solution of the Riemann problems RP($i-1, i$) and RP($i, i+1$). Note that for each cell i we only solve one Riemann problem, except for $i = 1$. Given the CFL condition (47), we sample the right half of the solution of RP($i-1, i$) if $0 \leqslant \theta_n < \frac{1}{2}$ or the left half of the solution of RP($i, i+1$) if $\frac{1}{2} \leqslant \theta_n \leqslant 1$. The sampling procedure itself, irrespective of the value of θ_n, has two main cases to consider, namely (A) the sampling point Q_i lies to the left of

Table I. Coefficients a_i and value of m when $k_1 = 2$ and $k_1 = 3$ for $n = 1$–10

	$k_1 = 2$					$k_1 = 3$			
n	a_0	a_1	a_2	a_3	m	a_0	a_1	a_2	m
1	1				0	1			0
2	0	1			2	2			1
3	1	1			2	0	1		2
4	0	0	1		3	1	1		2
5	1	0	1		3	2	1		2
6	0	1	1		3	0	2		2
7	1	1	1		3	1	2		2
8	0	0	0	1	4	2	2		2
9	1	0	0	1	4	0	0	1	3
10	0	1	0	1	4	1	0	1	3

Table II. (a) Coefficients A_i for sequence (3, 2) and (b) Van der Corput numbers (2, 1) and (3, 2) for $n = 1$–10

(a)				(b)	
n	A_0	A_1	A_2	θ_n for (2, 1)	θ_n for (3, 2)
1	2			0·0	0·1667
2	1			−0·25	−0·1667
3	0	2		0·25	−0·2778
4	2	2		−0·375	0·3889
5	1	2		0·125	0·0556
6	0	1		−0·125	−0·3889
7	2	1		0·375	0·2778
8	1	1		−0·4375	−0·0556
9	0	0	2	0·0625	−0·4259
10	2	0	2	−0·1875	0·2407

the contact discontinuity $dx/dt=u^*$ and (B) Q_i lies to the right of the contact discontinuity. Each case has two possible wave configurations. Figures 4 and 5 show these configurations for cases A and B respectively.

Consider case A, i.e. Q_i is to the left of $dx/dt=u^*$. The flow chart of Figure 6 shows the detailed sampling procedure. One proceeds to sample the wave pattern of Figure 4(a) if the left wave is a shock wave, i.e. $p^*>p_L$. Otherwise the wave configuration of Figure 4(b) is sampled (left rarefaction). For the shock case there are two possible regions, namely behind the shock (region star left) or in front of the shock (left state). For the rarefaction case there are three possible regions. If Q_i lies to the right of the tail of the rarefaction $dx/dt=u^*-c_L^*$, then we assign the solution corresponding to the region star left. If Q_i lies to the left of the head of the rarefaction $dx/dt=u_L-c_L$, then the data state $\mathbf{U}_L$ is assigned to the solution. Finally, if Q_i lies inside the rarefaction fan, the non-linear equation (40) must be solved to find ρ; the pressure p is found from equation (39) and the velocity u is found from equation (37).

Case B, where Q_i lies to the right of the contact discontinuity, is entirely similar to case A just described; it is its mirror image (see Figure 5).

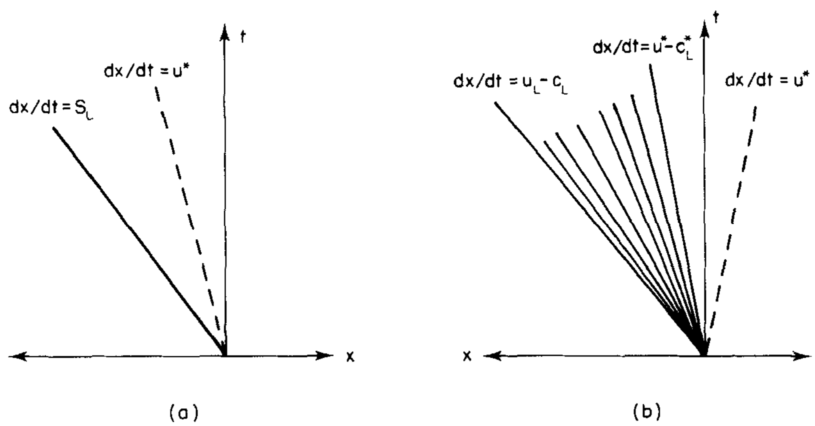

Figure 4. Wave configuration for case A where Q_i is to the left of the contact: (a) W_L is shock; (b) W_L is rarefaction

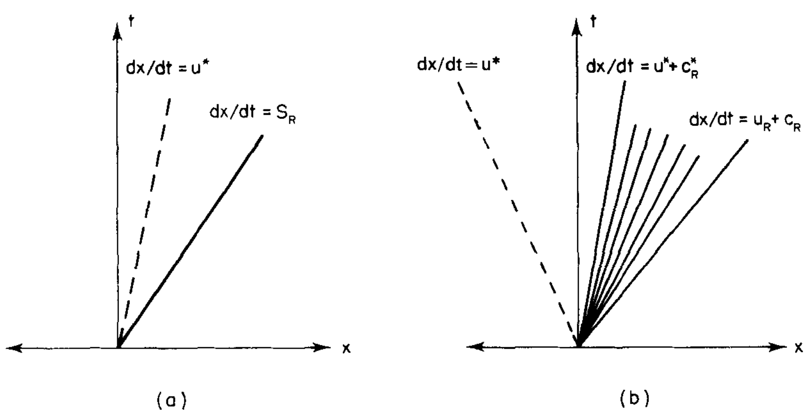

Figure 5. Wave configuration for case B where Q_i is to the right of the contact: (a) W_R is shock; (b) W_R is rarefaction

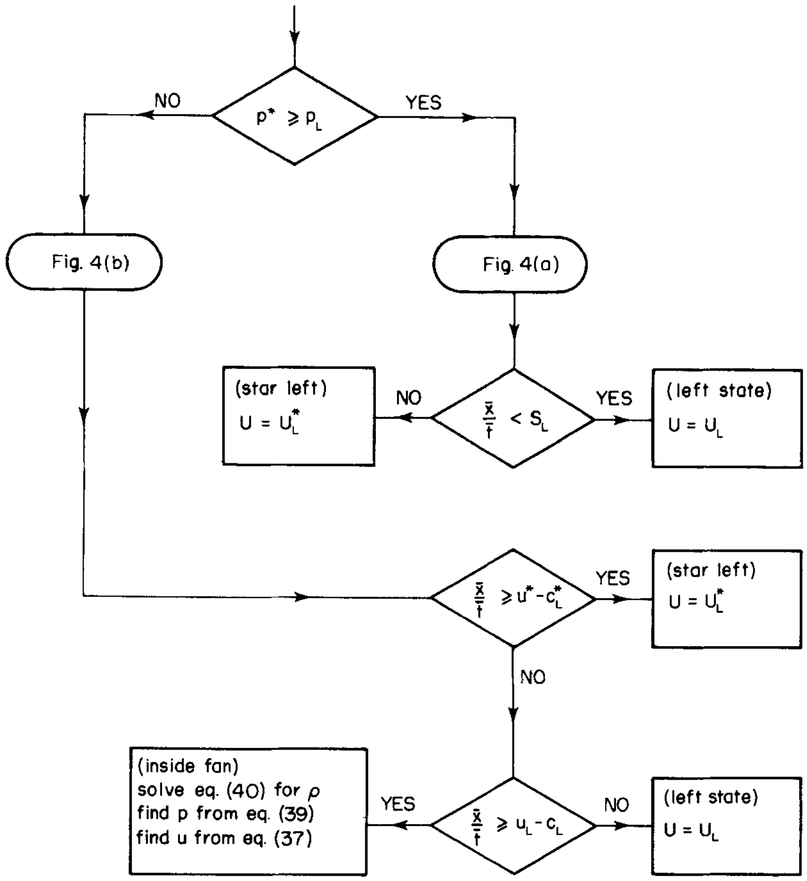

Figure 6. Sampling procedure for case A where Q_i lies to the left of the contact discontinuity $dx/dt = u^*$ (see Figure 4)

Table III. Data for two shock-tube problems

(a) Ideal case	(b) non-ideal case
$b = 0{\cdot}0$	$b = 0{\cdot}001\,(\mathrm{m^3\,kg^{-1}})$
$\gamma = 1{\cdot}4$	$\gamma = 1{\cdot}3$
$\rho_L = 1{\cdot}0$, $\rho_R = 0{\cdot}125$	$\rho_L = 100{\cdot}0$, $\rho_R = 1{\cdot}0(\mathrm{kg\,m^{-3}})$
$u_L = 0{\cdot}0$, $u_R = 0{\cdot}0$	$u_L = 0{\cdot}0$, $u_R = 0{\cdot}0(\mathrm{m\,s^{-1}})$
$p_L = 1{\cdot}0$, $p_R = 0{\cdot}1$	$p_0 = 100{\cdot}0$, $p_R = 0{\cdot}1(\mathrm{MPa})$
$x_0 = 0{\cdot}5$	$x_0 = 0{\cdot}4$

The application of the solution of the Riemann problem with covolume to the random choice method has been described. The resulting numerical technique to solve the one-dimensional unsteady Euler equations with general data and boundary conditions of practical interest can now be applied to a variety of problems in which covolume is important. Note that the present Riemann solver applies directly to the ideal-gas case ($b = 0$). Indeed, if covolume is not needed, then it is more efficient to exclude covolume in all equations.

In Reference 3 details of the ideal-gas algorithm are given, including FORTRAN programs for the Riemann solver and its implementation in the random choice method.

6. APPLICATIONS

Here we apply the solution of the Riemann problem with constant covolume to two classes of problems.

6.1. Shock-tube problems

Shock-tube problems are special cases of a Riemann problem and can therefore be solved exactly by direct application of the present Riemann solver. Also, as gas dynamic problems they can be solved approximately by solving the Euler equations numerically. This is done here by use of the RCM, which in turn utilizes, locally, the exact solution of the Riemann problem.

First, as a partial validation of the method, we solved the shock-tube problem with data as given in Table III(a). This is the ideal-gas case ($b=0$) and has a similarity solution. Figure 7 shows the results. They are coincident, as they should be. The second shock-tube problem is defined by the data of Table III(b). This is a case with covolume. Figure 8 shows a comparison between the ideal case ($b=0$) and the non-ideal case ($b=10^{-3}\ \mathrm{m^3\,kg^{-1}}$).

Differences are relatively small. The ideal-gas case gives a stronger shock but a weaker contact continuity. Also, the rarefaction for the ideal case is slightly weaker, but overall variations in ρ, u and p inside the rarefaction fan are small. Variations in internal energy are appreciable. This has implications for ignition criteria.

Figure 9 shows a comparison between the exact solution and the numerical solution (obtained by the RCM) of the covolume shock-tube problem.

Figure 10 shows the solution (using the RCM) for the shock-tube problem specified by Table III(a), but with covolume $b=0{\cdot}8$. This problem was solved numerically by Einfeldt[11] using an approximate Riemann solver. Obviously the value of b here is unrealistically high but serves the purpose of validating the present solution.

6.2. The Lagrange problem

The Lagrange problem[1] is essentially a moving-piston problem. This was solved exactly by Love and Pidduck[12] using the covolume (constant) equation of state with $b=0{\cdot}001\ \mathrm{m^3\,kg^{-1}}$. The problem is specified in Table IV. It consists of a long tube with a chamber region bounded at one end by a fixed boundary and with a movable piston of specified mass at the other end. Initial values are those simulating instantaneous combustion, but in a uniform state at time zero.

Figure 11 shows the numerical solution (full lines) and the exact solution (symbols) given by Love and Pidduck. The quantities are the piston travel, the piston velocity, the pressure at the fixed end of the chamber and the pressure at the base of the moving piston, all against time. The numerical solution was obtained by the random choice method using the exact solution of the Riemann problem with constant covolume locally. As observed in the figure, the agreement is excellent.

7. CONCLUSIONS

An efficient solver for computing the exact solution of the Riemann problem with the constant covolume equation of state has been presented. The pressure p^* between the acoustic waves is found by solving a single (non-linear) algebraic equation. The velocity u^* then follows directly.

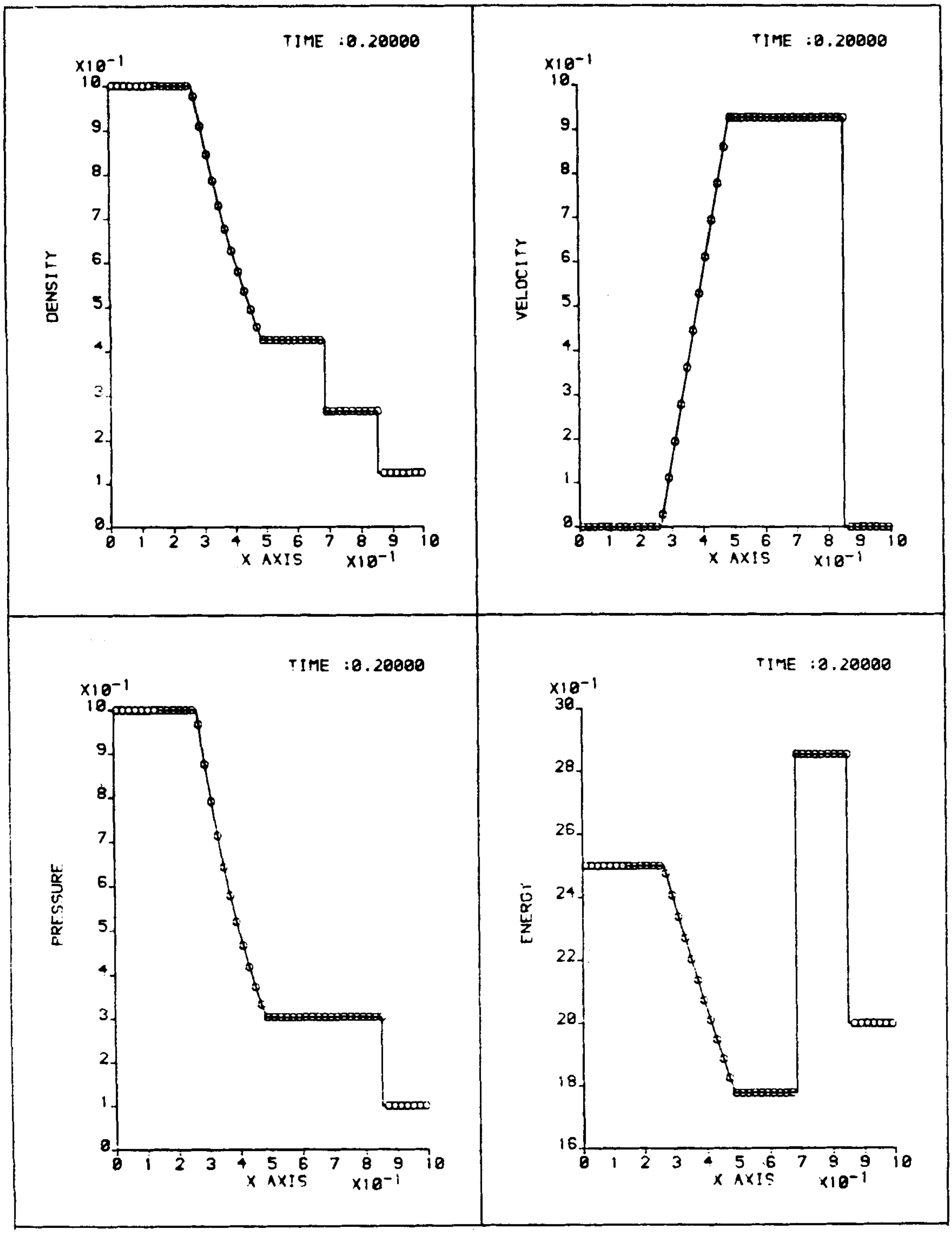

Figure 7. Sod's shock-tube problem. Present exact solution (symbols) and similarity solution (full lines)

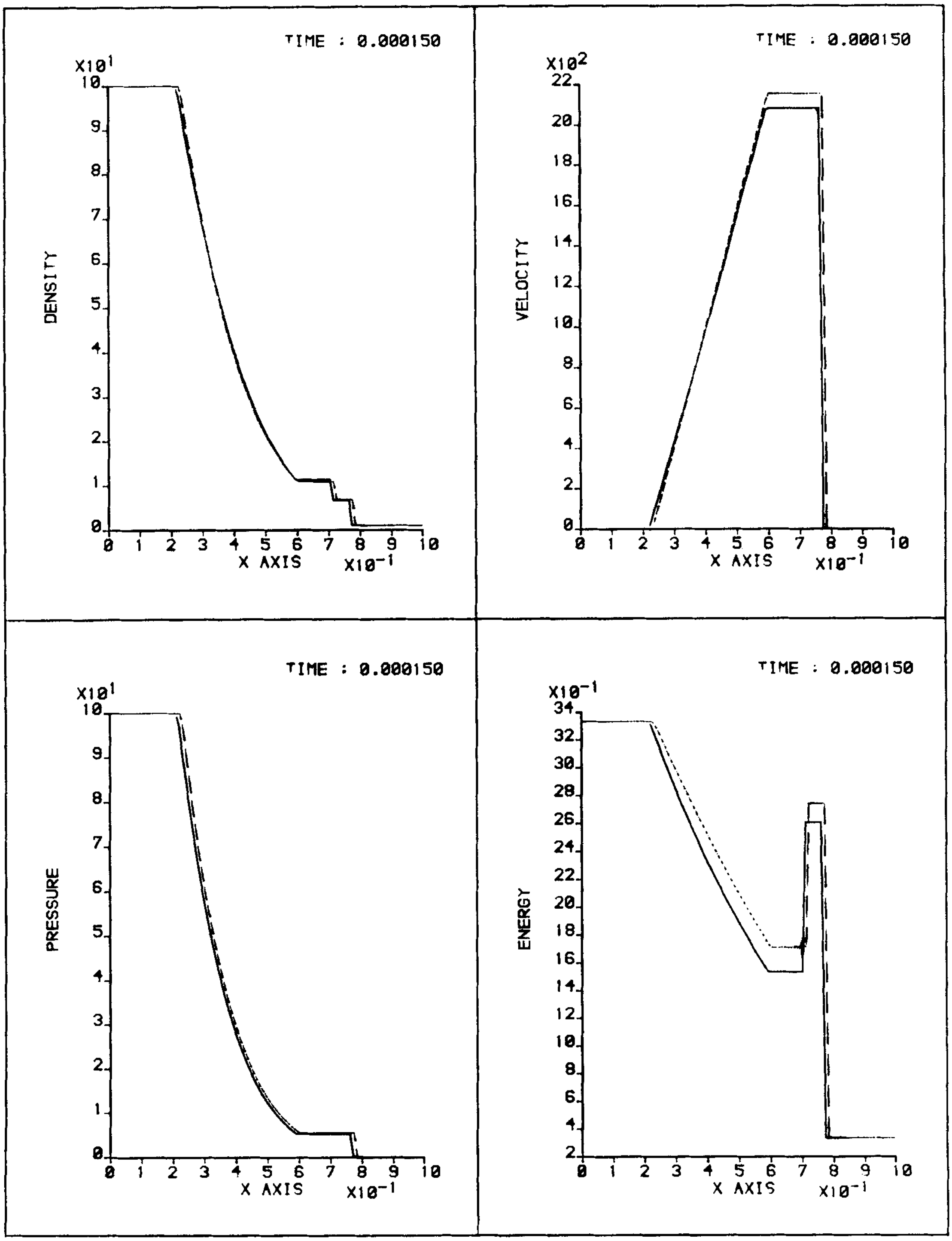

Figure 8. Shock-tube problems: exact solutions. Solution with covolume $b=0{\cdot}001$ (full lines) and ideal case $b=0$ (broken lines)

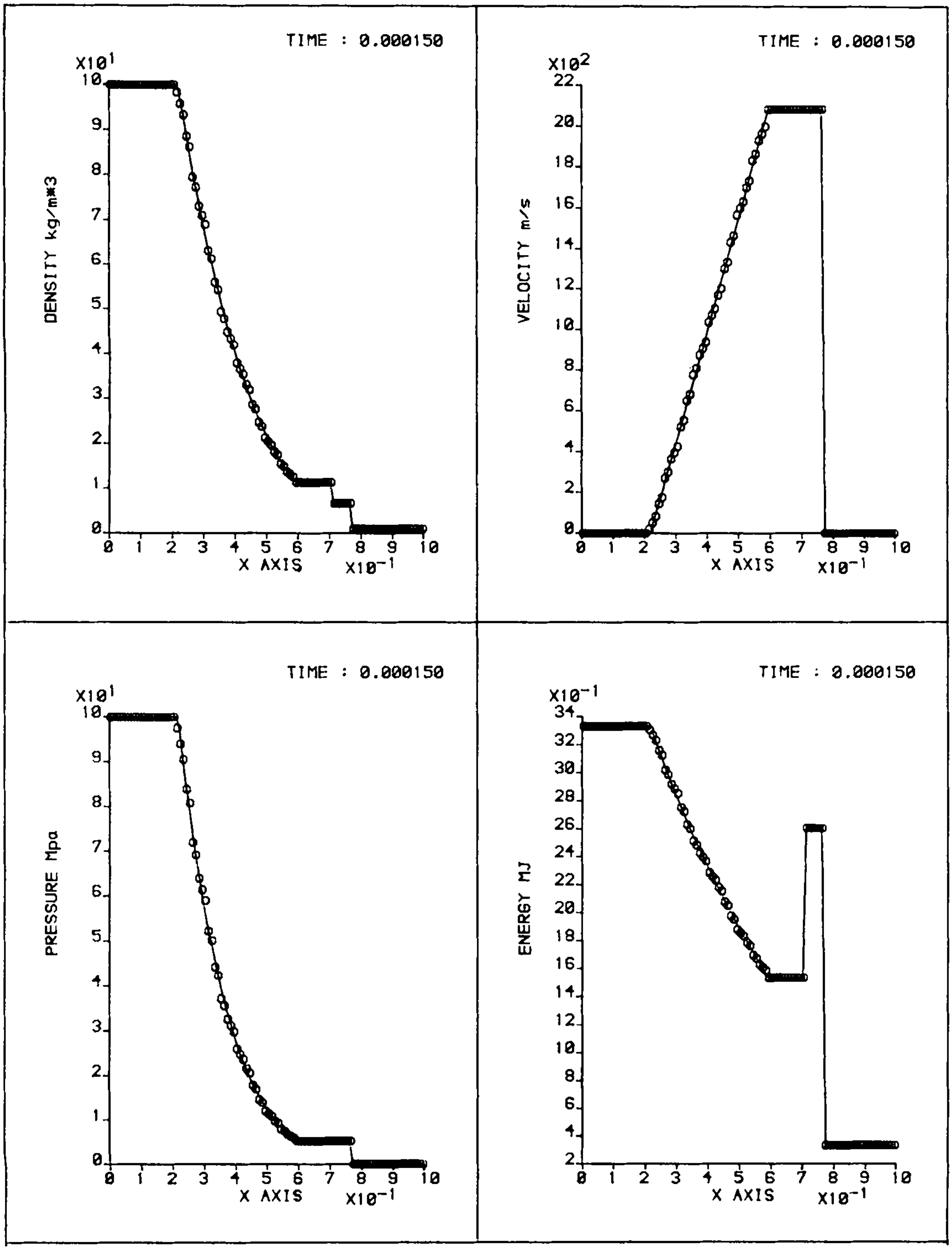

Figure 9. Shock-tube problem with covolume $b = 0{\cdot}001$. Computed solution by the random choice method (symbols) and exact solution (full lines)

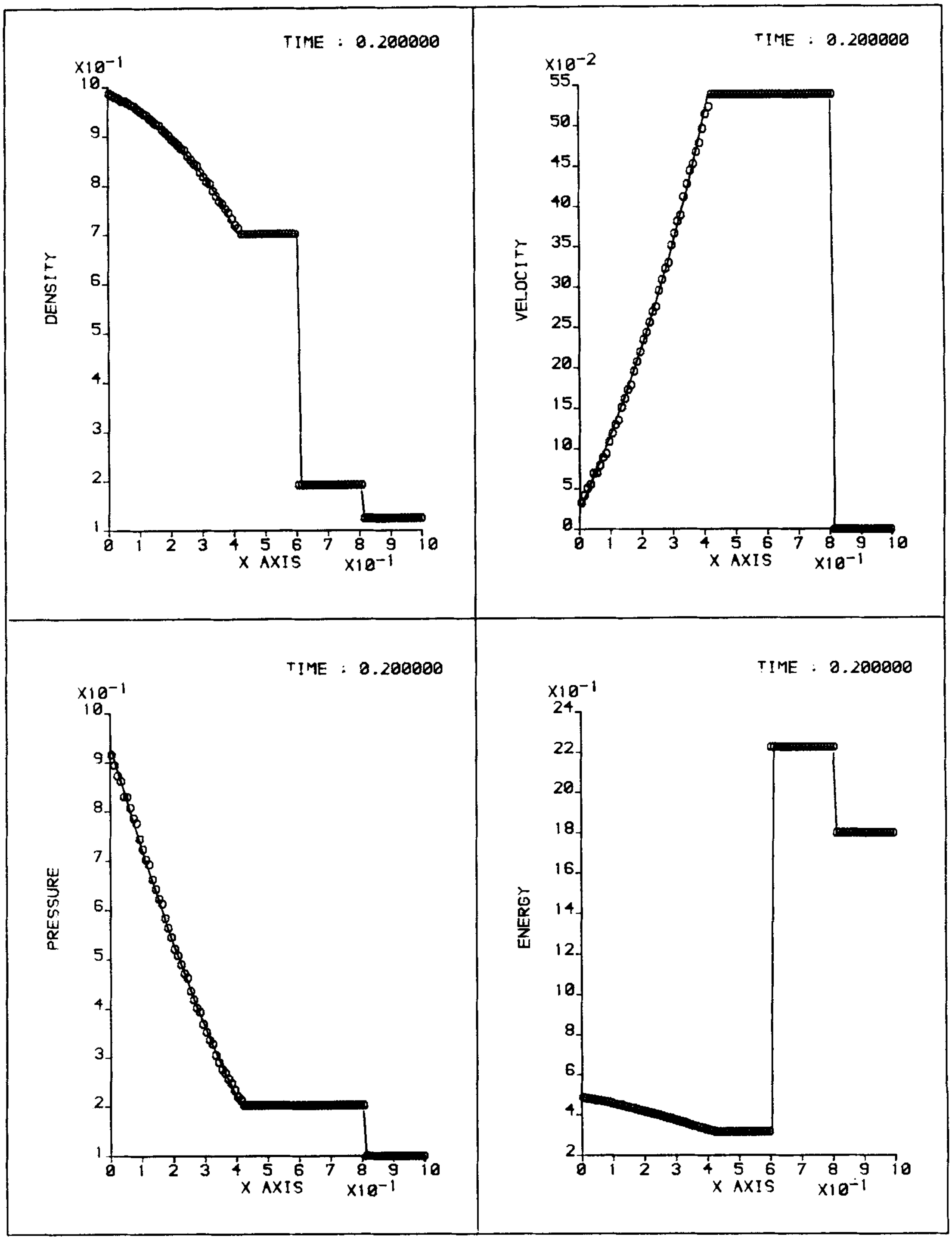

Figure 10. Einfeldt's shock-tube problem with $b=0{\cdot}8$. Computed solution by the random choice method (symbols) and exact solution (full lines)

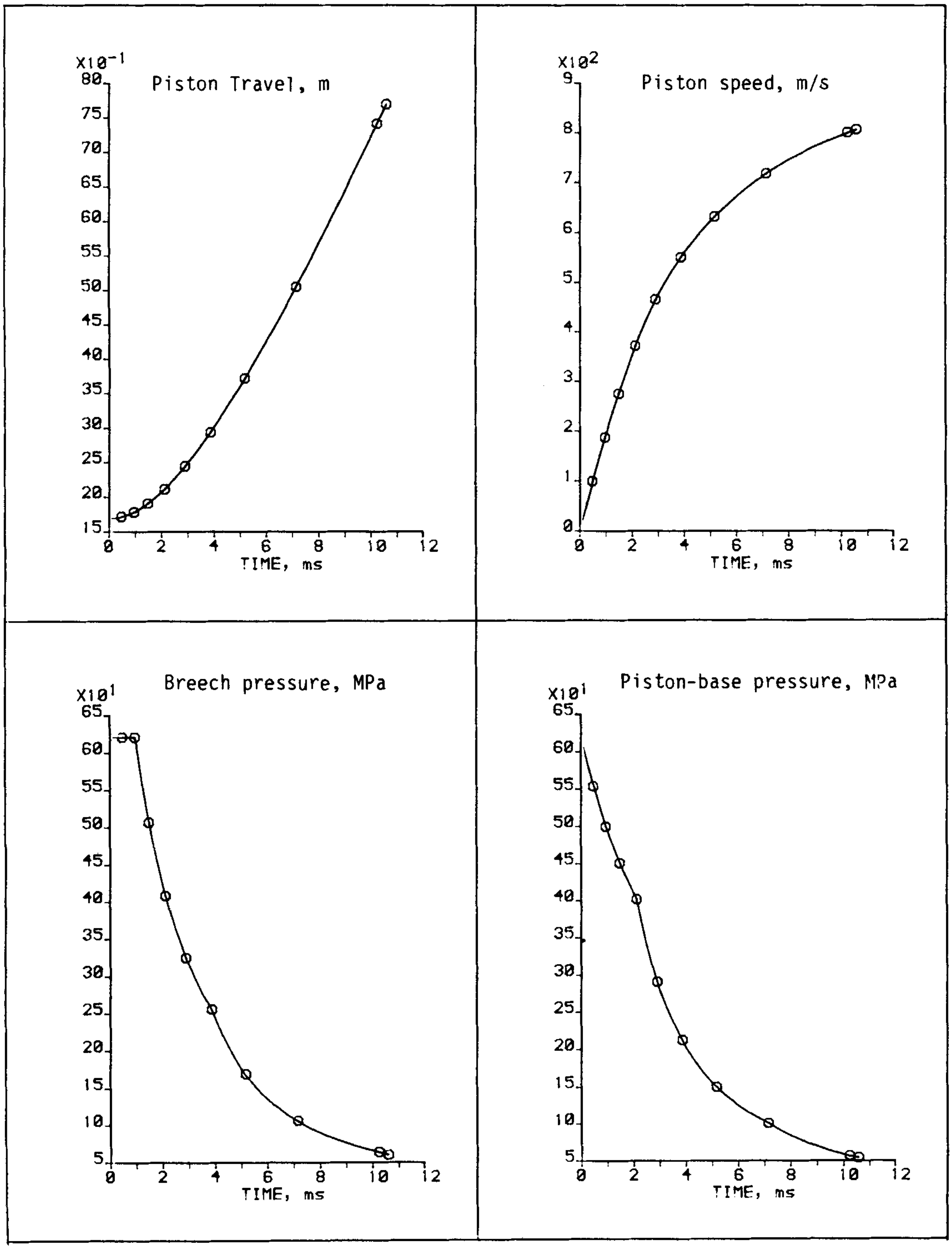

Figure 11. Lagrange's ballistics problem. Random choice solution for mesh $M_0 = 160$ (full lines) and exact solution (symbols)

Table IV. Parameters for the Lagrange problem

T_r, tube radius	0·075 m
l, total length of tube	7·698 m
l_c, length of chamber	1·698 m
p_0, initial pressure in chamber	621 MPa
ρ_0, initial gas density in chamber	400 kg m^{-3}
u_0, initial gas velocity in chamber	0·0 m s^{-1}
γ, ratio of specific heats	1·2222
b, covolume	0·001 m^3 kg^{-1}
m_p, mass of piston	12 kg

Values inside rarefaction fans require an extra iterative procedure for another single algebraic equation in ρ.

The solution is then incorporated into the random choice method, which is a numerical technique capable of solving the initial value problem with general initial data.

The solution is validated by direct application to shock-tube problems. The resulting RCM technique is also validated by solving shock-tube problems and the Lagrange problem.

REFERENCES

1. J. Corner, *Theory of the Interior Ballistics of Guns*, Wiley, 1950.
2. E. F. Toro and J. F. Clarke, 'Applications of the random choice method to computing problems of solid propellant combustion in a closed vessel', *CoA Report NFP 85/16*, Cranfield Institute of Technology, Cranfield, November 1985.
3. E. F. Toro, 'The random choice method on a non-staggered grid utilising an efficient Riemann solver', *CoA Report No. 8708*, Cranfield Institute of Technology, Cranfield, May 1987.
4. P. Collela, 'Glimm's method for gas dynamics', *SIAM J. Sci. Stat. Comput.*, **3**, 76 (1982).
5. R. Courant and K. O. Friedricks, *Supersonic Flow and Shock Waves*, Springer-Verlag, 1985.
6. A. Chorin, 'Random choice solutions of hyperbolic systems', *J. Comput. Phys.*, **22**, 517–536 (1976).
7. E. F. Toro, 'A new numerical technique for quasi-linear hyperbolic systems of conservation laws', *CoA Report No. 8626*, Cranfield Institute of Technology, Cranfield, December 1986.
8. E. F. Toro and P. L. Roe, 'A hybridised higher-order random choice method for quasi-linear hyperbolic systems', in H. Grönig (ed.), *Proc. 16th Int. Symp. on Shock Tubes and Waves*, Aachen, 26–30 July 1987, VCH publishers, pp. 701–708.
9. J. J. Gottlieb, 'Staggered and non-staggered grids with variable node spacing for the random choice method', Paper presented at *Second Int. Meeting on Random Choice Methods in Gas Dynamics*, Cranfield, 20–24 July 1987, *J. Comp. Physics*, **78** (1), 160–177 (1988).
10. J. M. Hammersley and D. C. Handscombe, *Monte Carlo Methods*, Chapman and Hall, 1964.
11. B. Einfeldt, 'On Godunov-type methods for the Euler equations with a general equations of state', in H. Grönig (ed.), *Proc. 16th Int. Symp. on Shock Tubes and Waves*, Aachen 26–30 July 1987, VCH publishers, pp. 671–676.
12. E. H. Love and F. B. Pidduck, 'Lagrange's ballistic problem', *Phil. Trans. R. Soc. London*, **222**, 167–228 (1922).